Monthly Notices
of the
ROYAL ASTRONOMICAL SOCIETY

MNRAS **493,** 1344–1351 (2020)
Advance Access publication 2020 February 4

doi:10.1093/mnras/staa329

On the possibility of through passage of asteroid bodies across the Earth's atmosphere

Daniil E. Khrennikov,[1] Andrei K. Titov,[2] Alexander E. Ershov,[1,3] Vladimir I. Pariev[4]★ and Sergei V. Karpov[1,5,6]★

[1]*Siberian Federal University, Svobodny Av. 79/10, Krasnoyarsk 660041, Russia*
[2]*Moscow Institute of Physics and Technology, Institusky Per. 9, Dolgoprudny 141700, Russia*
[3]*Institute of Computational Modeling SB RAS, Akademgorodok 50/44, Krasnoyarsk 660036, Russia*
[4]*P. N. Lebedev Physical Institute, Leninsky Prosp. 53, Moscow 119991, Russia*
[5]*L. V. Kirensky Institute of Physics, Federal Research Center KSC SB RAS, Akademgorodok 50/38, Krasnoyarsk 660036, Russia*
[6]*Siberian State University of Science and Technology, Krasnoyarsky Rabochy Av. 31, Krasnoyarsk 660014, Russia*

Accepted 2020 January 15. Received 2020 January 12; in original form 2019 June 28

ABSTRACT

We have studied the conditions of through passage of asteroids with diameters 200, 100, and 50 m, consisting of three types of materials – iron, stone, and water ice, across the Earth's atmosphere with a minimum trajectory altitude in the range 10–15 km. The conditions of this passage with a subsequent exit into outer space with the preservation of a substantial fraction of the initial mass have been found. The results obtained support our idea explaining one of the long-standing problems of astronomy – the Tunguska phenomenon, which has not received reasonable and comprehensive interpretations to date. We argue that the Tunguska event was caused by an iron asteroid body, which passed through the Earth's atmosphere and continued to the near-solar orbit.

Key words: meteorites, meteors, meteoroids – minor planets, asteroids: general.

1 INTRODUCTION

The problem of the motion in the Earth's atmosphere of a large space body (SB), capable of falling on to the surface of the planet in the form of meteorites, is now of great interest. An equally urgent concern is the study of the conditions for the passage of such bodies through the upper atmosphere, even without collision with the Earth's surface, since the shock waves produced by this passage have a colossal destructive effect (Loh 1963; Hawkins 1964; Martin 1966; Bronshten 1983; Tom Gehrels 1994; Stulov, Mirskiy & Vyslyi 1995; Nemchinov, Popova & Teterev 1999; Andruschenko, Syzranova & Shevelev 2013; Morrison & Robertson 2019; Robertson & Mathias 2019).

Large SBs (1–10 km in size and larger) that carry the potential danger of collision with the Earth are detected by ordinary astronomical observations. The bodies of intermediate dimensions began to be registered relatively recently. Observations of such bodies and the interpretation of observational data make it possible to determine the probability of their collision with the Earth, their properties, and the characteristic features of passage through the atmosphere, as well as the consequences of fall. The clarification of these questions will enable us to assess more accurately the degree of asteroid hazard.

One of the fundamental problems of meteor physics is the determination of the pre-atmospheric mass of SBs, since the intensity of the meteor phenomenon is determined by the kinetic energy of the body when entering the atmosphere of the planet. It is known that the velocity of the bodies belonging to the Solar system at the entrance to the Earth's atmosphere should be inside a relatively narrow range $11.2 < V_{sn} < 72.8$ km s^{-1} (Bronshten 1983), so that the variance of the contribution of the velocity-squared factor to the kinetic energy does not exceed 50 times. At the same time, the mass of a meteor body can vary in a much wider range: from fractions of a gram (micrometeor) to tens of millions of tons or more (the Tunguska space body), that is, by 13–15 orders of magnitude.

The goal of this paper is to evaluate the effect on the trajectory of the SB of its passage through dense layers of the atmosphere, taking into account the acting forces, the initial velocity, and the mass and its variation during the flight, to determine the conditions for possible passage of a large SB through the atmosphere with a minimum loss of mass without collision with the Earth's surface. The obtained results are compared with observational data on the Tunguska space body with an estimated altitude of maximum energy release of about 10–15 km to receive evidence in favour of a new explanation of the Tunguska phenomenon, which attributes the absence of meteoritic material on the Earth's surface near the epicentre to the through passage of the SB across the atmosphere with a small loss of velocity.

★ E-mail: vpariev@td.lpi.ru (VIP); karpov@iph.krasn.ru (SVK)

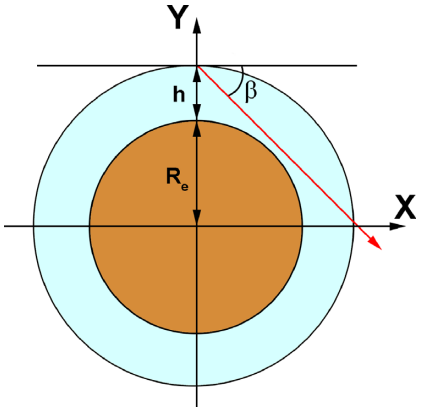

Figure 1. Schematic diagram of the motion of a space body in the Earth's atmosphere and the angle of entry into the atmosphere (β) at a given point relative to the X–Y coordinate system. R_e is the radius of the Earth. Thickness of the atmosphere is exaggerated. The trajectory of SB and its length within the atmosphere are indicated by the line with the arrow.

2 PHYSICAL MODEL

First of all, let us imagine a model explaining the entry of the SB into the Earth's atmosphere with respect to the chosen X–Y coordinate system coinciding with the centre of the Earth and corotating with the rotation of the Earth (Fig. 1). The altitude of the entry of the SB into the atmosphere is measured from the starting value $h = 160$ km, at which the temperature of the SB begins to increase (Bronshten 1983). This layer of the atmosphere is indicated in Fig. 1 by the value of h (the same parameter denotes the current altitude of SB over the Earth's surface). The angle of entry into the atmosphere relative to the local horizontal line at the altitude h is one of the most important parameters of the problem and is denoted by β. We denote by L the length along the curved trajectory of SB in the atmosphere, $\mathrm{d}L = \sqrt{\mathrm{d}X^2 + \mathrm{d}Y^2}$, and $L = 0$ corresponds to the entry point of the SB into the atmosphere at $h = 160$ km.

2.1 The equation of motion with a variable mass

Ballistics of the SB are described by a system of equations, including the equation of motion under the action of applied forces: the force of the aerodynamic drag F_f and the gravitational force $\boldsymbol{F}_g = M\boldsymbol{g}$ (Stulov et al. 1995):

$$M\frac{\mathrm{d}\boldsymbol{V}}{\mathrm{d}t} = -\frac{1}{2}c_\mathrm{d}\rho_h V^2 S\frac{\boldsymbol{V}}{V} + M\boldsymbol{g},$$
$$\boldsymbol{g} = -\frac{GM_\mathrm{e}}{r^3}\boldsymbol{r}, \quad \frac{\mathrm{d}\boldsymbol{r}}{\mathrm{d}t} = \boldsymbol{V}. \tag{1}$$

Here M is the mass, $\boldsymbol{V}$ is the velocity of the body relative to the Earth, t is time, G is the gravitational constant, g is the acceleration of gravity, M_e is the mass of the Earth, c_d is the drag coefficient, and ρ_h is the density of the atmosphere at altitude h (NASA 1976). S is the area of the body's middle cross-section, $\boldsymbol{r}$ is the current radius vector, and r is the absolute value of the current radius vector (the distance from the SB to the centre of the Earth). The time dependence of M is implied in equations (1)–(3).

We note that the contribution of the lifting force to the ballistic of the SB is also neglected in equation (1) because we assume that the shape of the SB is close to spherical. The Coriolis and centrifugal forces in the rotating reference frame are negligible for fast-moving SBs compared to the aerodynamical forces from stratospheric winds, which we also neglect here because SBs move much faster than the wind speed.

In accordance with the existing ideas, e.g. Stulov et al. (1995), the main contribution to the force of aerodynamic drag is made by the difference in pressure between the frontal and rear parts of the SB surface (low-pressure cavity forms near the rear surface). The expression for the force of aerodynamic drag corresponds to the first term in equation (1). The area S depends on the current mass and size of SB (equation 2). In equation (2), the initial values of the cross-sectional area and the mass of the SB are indicated as S_0 and M_0:

$$S(t, M) = S_0\left(\frac{M(t)}{M_0}\right)^{\mu}. \tag{2}$$

We apply the simplified approach of isotropic loss of material from the SB surface, which corresponds to the case $\mu = 2/3$. Determining the exponent μ is the subject of a separate study (Bronshten 1983) taking into account the complexity of the problem in a general case. The dependence $S(t, M)$ is used in the numerical solution of the differential equation (1) at each time iteration step together with the change in the SB mass (see equation 3).

The value of the SB drag coefficient (Kutateladze 1990), in a general case, depends on the Reynolds number $Re = \frac{VR}{\nu}$, where R is the radius of SB and ν is the kinematic viscosity of the air. At a velocity in the range $10 < V < 40$ km s^{-1}, the radius of SB is of the order of several dozens of metres, kinematic viscosity of air at a trajectory altitude is of the order of 5×10^{-5} m^2 s^{-1} and greater. Therefore, the Reynolds number exceeds 10^{10} (Bronshten 1983). According to Kutateladze (1990), Spearman & Braswell (1993), and Zhdan et al. (2007), if the Reynolds number exceeds the value 1.5×10^5, then a sharp drop of c_d to 0.1 with a subsequent raise on average of up to 0.9–1 takes place. In our case, the value of $c_\mathrm{d} = 0.9$ corresponds to the most extreme conditions for the motion of spherical SB in the atmosphere.

2.2 The loss of the space body mass and the heat transfer with the shock wave boundary layer

The following equation describes the loss of SB mass when moving in the atmosphere:

$$\frac{\mathrm{d}M}{\mathrm{d}t} = -\frac{c_\mathrm{h}\rho_\mathrm{h}V^3 S}{2H}. \tag{3}$$

Here H is the specific heat of sublimation of the SB material and c_h is the coefficient of radiation heat transfer, defined as the fraction of the kinetic energy of the oncoming stream of molecules that goes into the sublimation of the SB material (Bronshten 1983).

Mass-loss of SB occurs due to heating to a temperature much higher than the melting point (Stulov et al. 1995). In our case, the main contributor to this heating is the radiant heat transfer between the SB and the boundary layer of the shock wave, whose temperature reaches several thousand degrees close to the surface of the SB (Bronshten 1983). One of the most difficult problems in calculating the radiant heat transfer is the determination of the radiant heat transfer coefficient (c_h). Its magnitude is affected by the velocity of motion in the atmosphere, flight altitude, air density, temperature of the boundary layer and the nature of the processes in the boundary layer (dissociation and ionization of air molecules), the degree of blackness of the radiating and absorbing surfaces, etc. According to the available data, depending on the altitude and the SB velocity, the values of the radiant heat transfer coefficient lie in the range $0.01 \leq c_\mathrm{h} \leq 0.1$ (Svetsov, Nemtchinov & Teterev 1995;

Andruschenko et al. 2013; Johnson, Stern & Wheeller 2018) (the maximum value is reached at an altitude of about 10 km). Taking into account that the mass-loss rate reaches a maximum at $c_h = 0.1$, this value will be used in further calculations. According to Svetsov et al. (1995), this value gives the best fit with observational data. The degree of blackness for the radiating and absorbing surfaces was taken to be equal to 1 in the calculations because of the high temperature of the surfaces and the formation of a dense high-temperature plasma (Bronshten 1983). The solution of the system of differential equations (1) and (3) together with algebraic equation (2) was carried out by the explicit Runge–Kutta method of the fourth order.

Note that the employed model does not involve the process of SB fragmentation (Stulov & Titova 2001; Barri 2010; Dudorov et al. 2015), since the initial dimensions of the SB are taken to be quite significant (from 50 to 200 m) as well as moderate velocities, when most of the SB remains intact, despite extreme external influences. First of all, maximum resistance to fragmentation is characteristic of iron SBs, which is associated with the high homogeneity of their internal structure. In contrast to the iron SBs, the internal structure of stone and ice SBs is heterogeneous with an abundance of numerous microcracks. The results of the study of the conditions for the fragmentation of iron SBs will be presented in our next paper.

We denote the mass-loss by the term 'ablation', which includes two processes: The first process is the low-temperature blowing off a liquid film from the SB surface (at a temperature about 1000°C) with the formation of small droplets. These droplets are typical for a slow fall of small SBs or their fragments at the final stage of the flight in the atmosphere. The second process is the high-temperature sublimation of material occurring when the surface temperature exceeds several thousand degrees. In this case, a mass-loss occurs in the form of vapours of single atoms and their ions. Under the conditions in consideration, the employed model includes the sublimation as a dominant process responsible for the mass-loss at high velocities – over 11.2 km s^{-1}.

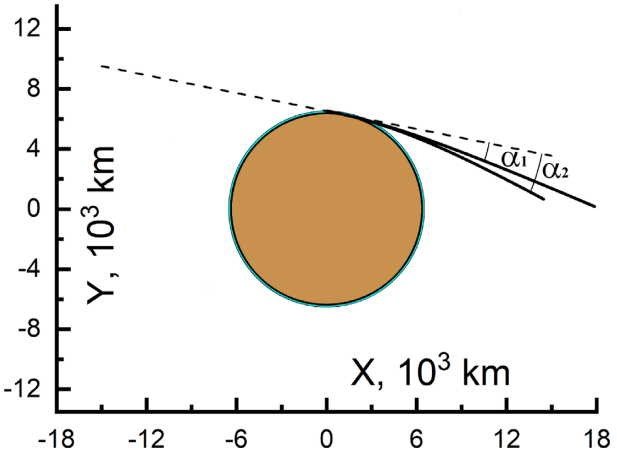

Figure 2. Changes in the trajectory of SB during a through passage via the atmosphere. The SB parameters are radius $R = 50$ m, the velocity of entry into the atmosphere is 20 km s^{-1}, and the minimum altitude is 11 km. The angle of deflection $\alpha_1 = 11.^\circ25$ at $c_d = 0$ and $\alpha_2 = 16.^\circ9$ at $c_d = 0.9$. The trajectory lengths correspond to the time moment 1000 s after the entrance into the atmosphere.

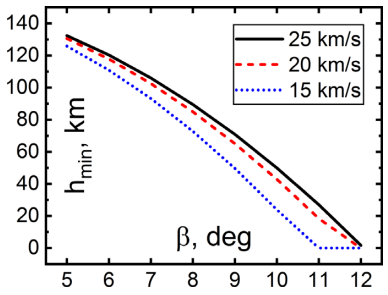

Figure 3. Dependence of the minimum trajectory altitude on the entry angle for the $R = 100$ m iron SB at different velocities.

3 RESULTS AND DISCUSSION

As a typical example of our calculations, Fig. 2 illustrates the results of calculating the trajectory of the spherical iron SB with a radius $R = 50$ m entering into the atmosphere at 20 km s^{-1} when passing through it at the entry angle $\beta = 11.^\circ2$ and a minimum altitude of 11 km. As can be seen from this figure, the perturbation of the trajectory of the SB deviates it from the initial direction by an angle $\alpha_1 = 11.^\circ25$ when neglecting the aerodynamic drag effect and $\alpha_1 = 16.^\circ9$ when the aerodynamic drag effect is taken into account. These results demonstrate the significant effect of aerodynamic drag on the SB trajectory.

Fig. 3 shows the dependence of the minimum trajectory altitude for iron SBs with $R = 100$ m on the angle of entry into the atmosphere for three velocities. Calculations did not reveal significant differences for the SBs with radii $R = 100$, 50, and 25 m.

The complex pattern of aerodynamic fluxes around a spherical SB, vortex formation, and stagnation zone in its rear part are shown in Fig. 4. This figure demonstrates the extreme conditions for the passage of a spherical SB through the dense layers of the atmosphere as well as clearly shows the conditions for the occurrence of the aerodynamic drag taking into account the structure of fluxes in the stagnation zone. The results illustrated in Fig. 4 were obtained with the software package ANSYS FLUENT (Hutton 2017). This package is a universal software system of the finite-volume method applied for solving various problems in aero- and hydrodynamics (Hutton 2017). To calculate the pressure distribution at the surface of an SB with the effect of air compression due to pressure–density dependence, the FLUENT 'ideal gas' model was used with the laminar flow regime. Zero static pressure was set to absolute pressure 26 500 Pa at an altitude of 10 km (NASA 1976). The default air temperature was set to 219 K.

Fig. 5 shows the trajectories of an SB at different angles of entry into the atmosphere corresponding to the passage of SBs through the atmosphere at different minimum altitudes over the Earth's surface.

In this section, we present the results of calculations for bodies of several sizes, consisting of iron, stone, and ice. Calculations were carried out for the values of the radii of the SBs with $R = 25$, 50, and 100 m and for three materials: For iron, the specific heat of sublimation of iron is $H = 6380$ kJ kg^{-1} (Luchinsky 1985), for stone, $H = 3965$ kJ/kg for a specimen of lunar rock (Ahrens & O'Keefe 1971) and $H = 9300$ kJ kg^{-1} for quartz (Chirikhin 2011), and for water ice, $H = 2853$ kJ kg^{-1} (Voitkovskiy 1999). In calculations with a stone SB, we used a larger value of H for quartz, since SiO_2 is the basis of many natural minerals. The use of a smaller value of H (3965 kJ kg^{-1} for lunar rock) results in an increase in the mass-loss of stone SBs.

Figs 6 and 7 illustrate the mass-loss of an iron SB and its rate when it is moving through the atmosphere at different velocities and at a minimum trajectory altitude of 11 km. This altitude lies

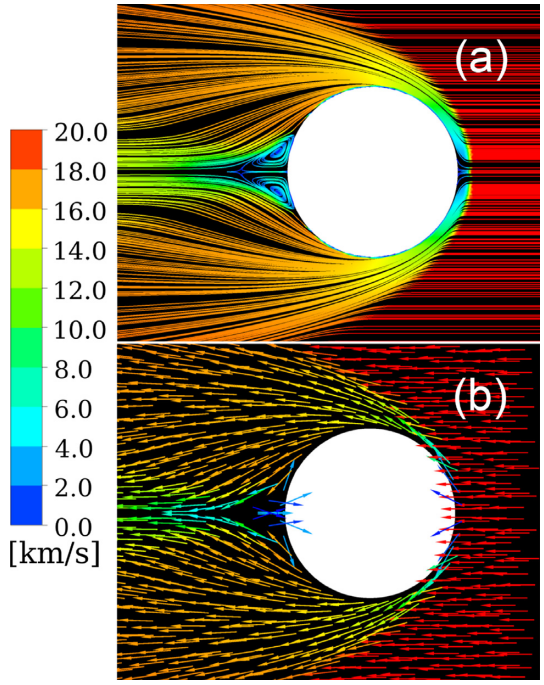

Figure 4. (a): Distribution of the velocity modulus around a spherical SB with radius $R = 100$ m; and (b): distribution of the velocity vectors.

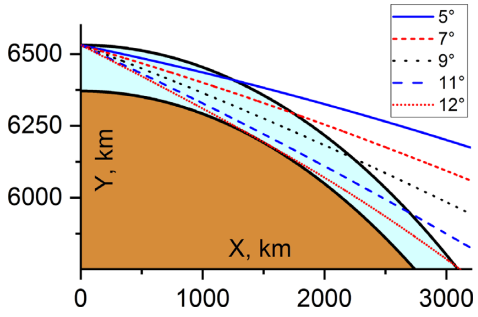

Figure 5. The trajectories of the passage of SB through the atmosphere at entry angles (β) in the range 5°–12°. Material is iron, radius of SB is $R = 100$ m, and initial velocity is 25 km s^{-1}.

in the range of generally accepted values of the minimum altitude for the Tunguska space body: 10–15 km (e.g. Bronshten 1983). These dependencies are affected both by the velocity of SB, which increases the loss of material, and by the time of flight through the atmosphere, which reduces this loss.

Besides less loss of mass at lower velocity (15 km s^{-1}), we can see the effect of lengthening of trajectory in the atmosphere from 3000 to 5000 km, which takes place for smaller size SBs as well (Fig. 6f).

The main results of our calculation are presented in Table 1, which can be considered as upper estimates of the residual masses of SBs for different sizes and materials after through passage of the Earth's atmosphere for a trajectory length of 3000 km. As can be seen from Table 1, the maximum fraction of the preserved mass is observed in the iron SBs with a radius of 100 m at lower initial velocities. When the velocities grow, the residual mass falls considerably. Similar tendencies are observed for the stone SBs (without regard to their fragmentation) with a significantly greater relative mass-loss. For the case of ice SBs, at initial velocities higher than 15 km s^{-1}, a

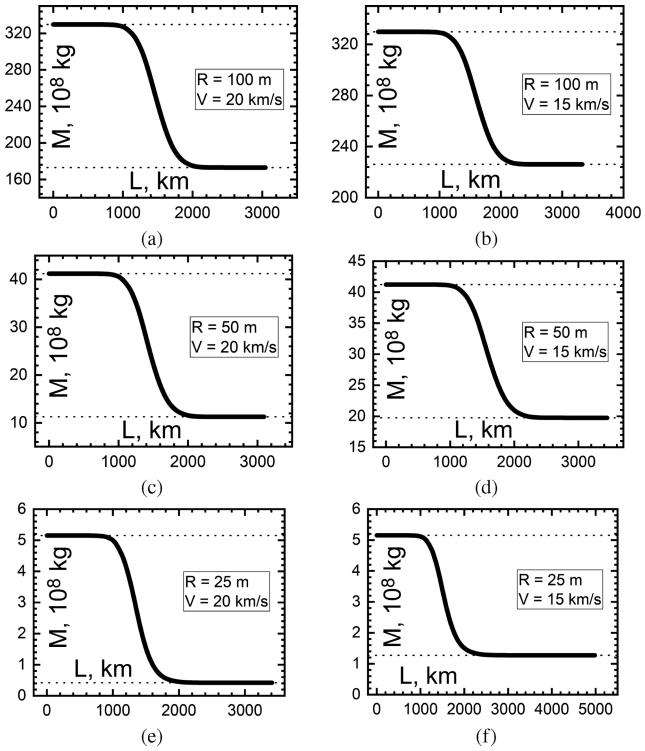

Figure 6. Change in the residual mass of the iron SBs [$M(L)$] along the trajectory through the atmosphere at two values of initial velocities and for three SB radii. L is the length along the trajectory measured from the entry point into the atmosphere at altitude $h = 160$ km. The curves end when the SB reaches the exit point from the atmosphere at the same altitude $h = 160$ km. The minimum altitude $h_{\min} = 11$ km and $c_d = 0.9$.

complete loss of mass may take place. A faster mass-loss of stone SBs compared to iron SBs of the same size is associated with a lower mass of stone SBs due to much lower material density. That is, if the amount of absorbed energy from the boundary layer of shock wave is the same for equal sizes, then the fraction of the lost mass (relative to the initial one) will be greater for the stone SB compared to the iron one. Complete loss of mass of the ice SBs at any initial velocities and sizes is explained by their low mass due to low ice density. Another reason is a low specific heat of sublimation of ice. Larger minimum altitudes of trajectory in calculations ($h_{\min}$) indicated in the table caption for stone and ice SBs were used to prevent these SBs from falling.

Fig. 8 illustrates the variation of the velocity of SBs along the trajectory with radii $R = 100$, 50, and 25 m. The calculations were carried out with drag coefficient $c_d = 0.9$ for a spherical body. The obtained results show that the smaller the SB size, the higher the deceleration. There is a more notable decrease in SB velocity with a radius of 25 m in comparison with the radii of 100 and 50 m. Fig. 8 contains a very important result for further consideration, reflecting our conclusion that this dependence lies in the basis of the mechanism of the SB tail formation when the fragmentation of the SB occurs – the smaller the fragment and the lower its kinetic energy, the greater its deceleration and the lower its final velocity compared to larger fragments.

Fig. 9 demonstrates the changes in trajectories of the iron SB with $R = 25$ m passing through the atmosphere with initial velocities 20 and 15 km s^{-1} and the effect of lengthening of the trajectory from 3000 to 5000 km at slower velocity and a minimum trajectory altitude of 11 km. Both SBs exit the atmosphere but at different

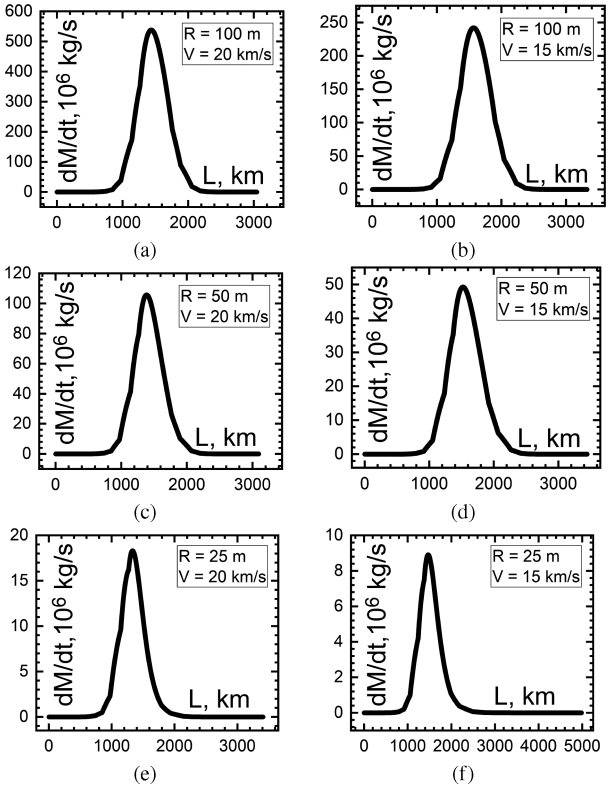

Figure 7. Change in the rate of the mass-loss of the iron SBs [d$M(L)$/dt] along the trajectory through the atmosphere at two different initial velocities and for three SB radii. The curves end when the SB exits from the atmosphere at altitude $h = 160$ km. The minimum altitude $h_{\min} = 11$ km and $c_{\rm d} = 0.9$.

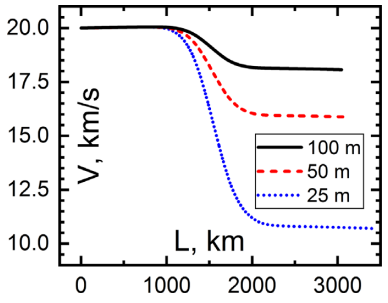

Figure 8. Changes in the velocity of the iron SBs along the trajectory when passing through the atmosphere for the radii $R = 100$, 50, and 25 m at a minimum altitude of 11 km ($c_{\rm d} = 0.9$). The curves end when the SB exits from the atmosphere at an altitude $h = 160$ km.

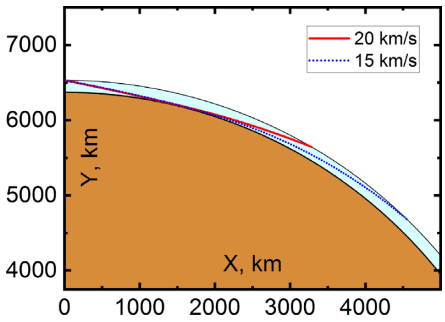

Figure 9. Difference in the iron SB trajectories with radius $R = 25$ m when passing through the atmosphere with two different initial velocities and a minimum altitude of 11 km ($c_{\rm d} = 0.9$).

moments of time. The effect of lengthening of the SB trajectory is also shown in Fig. 6.

4 APPLICATION OF THE THROUGH PASSAGE MODEL TO THE TUNGUSKA PHENOMENON

At present, there are over 100 hypotheses about the nature of the Tunguska phenomenon, among which three to four versions are predominant theories (e.g. Fesenkov 1962; Bronshten 2000a; Farinella et al. 2001; Kundt 2003; Gladysheva 2008). They include the fall on to the Earth of a small asteroid measuring several dozen metres (Kundt 2003), consisting of typical asteroid materials, either metal or stone, as well as ice, which is characteristic of cometary nuclei (Fesenkov 1962; Bronshten 2000b; Morrison & Robertson 2019). The most probable material of the Tunguska SB mentioned in literature is ice. According to the available observational data, there are several variants of the direction and the trajectory length of the Tunguska SB – from 450 to 600 km, in particular, with a propagation direction from 'south–north' to 'east–west'. The value of the angle of entry into the atmosphere mentioned in literature is 30°–40°. The radius of the Tunguska SB was estimated based on the amplitude of the shock wave recorded by the seismic stations and amounted to about 25 m. The minimum trajectory altitude of the Tunguska SB approximately corresponded to the point of maximum energy release.

In Fig. 10, we show the results of comparative calculations of the velocity variations of the iron, stone, and ice SBs with radii 100 and 50 m along the trajectory of through passage across the atmosphere for an initial velocity of 20 km s^{-1}. Stone SBs lose their velocity faster than iron SBs and ice SBs do not survive passage through the atmosphere.

In Fig. 11, we demonstrate an unusual trajectory of a stone SB with $R = 50$ m compared to an iron one with the same size. At point 1, the SB penetrates the atmosphere at altitude 160 km, at point 2, it reaches the minimum altitude of 11 km, at point 3, it exits the atmosphere at altitude 160 km with a subsequent re-entry due to a significant decrease in velocity, and at point 4, it is near the point of fall. There is a considerable lengthening of trajectory of the stone SB compared to the iron body, which passes through the atmosphere

Table 1. The ratios of the preserved mass of SB $M_{\rm out}$ to the initial mass $M_{\rm in}$ for different materials at different initial velocities V and initial sizes R. Calculations are performed for minimum altitude $h_{\min} = 11$ km, except for the stone SB with $R = 25$ m ($h_{\min} = 18$ km), and for the ice SBs with radii $R = 100$, 50, and 25 m with corresponding $h_{\min} = 18$, 23, and 28 km.

Material	Iron			Stone			Ice		
R (m)	100	50	25	100	50	25	100	50	25
$M_{\rm out}/M_{\rm in}$ ($V = 15$ km s^{-1})	0.69	0.48	0.25	0.49	0.32	0.3	0.017	0.014	0.01
$M_{\rm out}/M_{\rm in}$ ($V = 20$ km s^{-1})	0.52	0.27	0.08	0.298	0.11	0.1	0	0	0

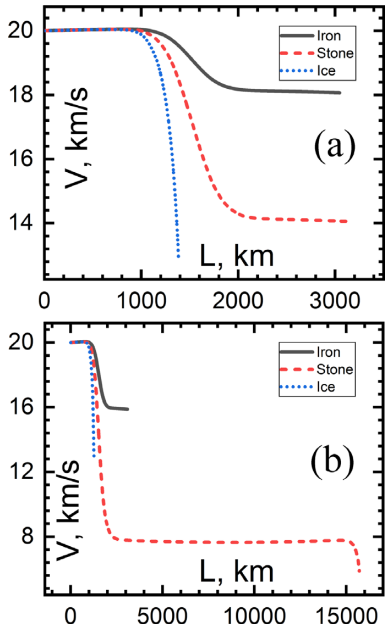

Figure 10. Comparative variation of the velocity of the iron, stone, and ice SBs along the trajectory with $R = 100$ m (a) and $R = 50$ m (b). The initial velocity 20 km s^{-1} and the minimum trajectory altitude is 11 km. The curves for iron and stone SBs in panel (a) end when the SB exits the atmosphere at an altitude $h = 160$ km. The curves for ice SBs end when the mass of the SBs vanishes completely. The long curve for the stone SB in panel (b) corresponds to an unusually long trajectory of the stone SB shown in Fig. 11.

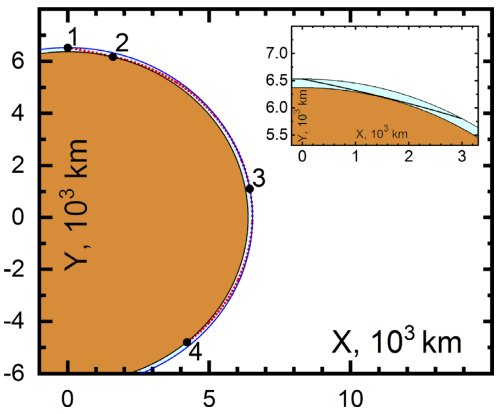

Figure 11. The trajectory of a stone SB with radius $R = 50$ m. Initial velocity is $V = 20$ km s^{-1} and minimum altitude is 11 km. At point 1: $V = 20$ km s^{-1}, relative mass $M/M_{in} = 1$, and $h = 160$ km; at point 2: $V = 14.2$ km s^{-1}, $M/M_{in} = 0.3$, and $h = 11.26$ km; at point 3: $V = 7.6$ km s^{-1}, $M/M_{in} = 0.13$, and $h = 159.7$ km; at point 4: $V = 5.9$ km s^{-1}, $M/M_{in} = 0.11$, and $h = 11$ km (with a subsequent fall). The inset shows the comparison of trajectories of the stone and iron SBs with an equal radius $R = 50$ m.

with a minimum loss of velocity and minimum deflection due to a high initial mass (its trajectory is shown in the inset). Although quite improbable, such an SB could manifest itself as a pair of explosive phenomena in the atmosphere separated by thousands of kilometres in distance and tens of minutes in time.

Fig. 12 shows trajectories of an ice SB with $R = 100$ m at different entry angles and changes in mass. This figure demonstrates

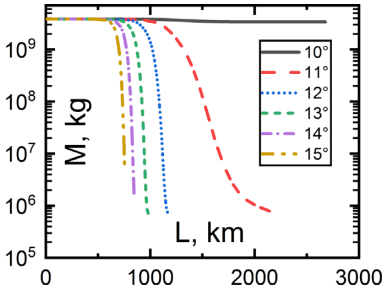

Figure 12. Variation of the ice SB mass along the trajectory with an initial velocity 20 km s^{-1} and an entry angle in the range $10° \leq \beta \leq 15°$ for different minimum altitudes of the trajectory. The initial SB radius is 100 m.

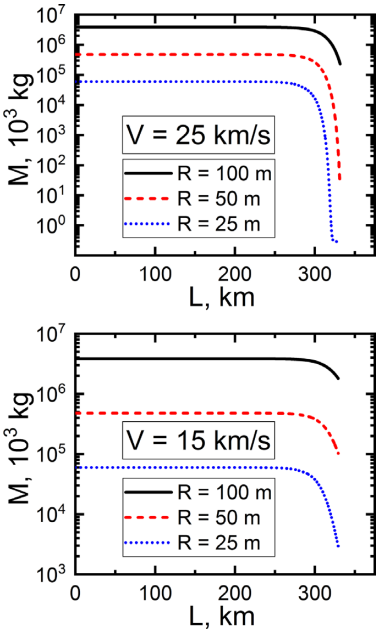

Figure 13. Variation of the ice SB mass along the trajectory of fall with an initial velocity 25 and 15 km s^{-1} and entry angle 30°.

a dramatic loss of mass at angles over 11°. At angle 10°, the initial mass is preserved due to the high altitude – over 50 km (Fig. 3).

Fig. 13 shows the reduction of the masses of ice SBs with $R = 100$, 50, and 25 m on the trajectory of collision with the surface of the Earth. The residual fractions of the mass at an initial velocity of 15 km s^{-1} are 49 per cent, 21.3 per cent, and 4.8 per cent, respectively, for radii $R = 100$, 50, and 25 m of the SBs. The length of the trajectory until the moment of the collision with the surface of the Earth is about 325 km for the initial velocity of 15 km s^{-1}. At an entry velocity of 25 km s^{-1} for radii $R = 100$ and 50 m, SBs fall with a preservation of 6 per cent and 0.000 04 per cent of the initial mass respectively. For radius $R = 25$ m and entry velocity of 25 km s^{-1}, an ice SB loses all its mass completely within a trajectory length of about 329 km.

Of course, the fall of SB with preservation of a significant part of the initial mass results in the formation of a crater with a diameter larger than 1 km (Stulov et al. 1995). But the fact is that there are no craters near the epicentre and around. The actual length of the trajectory based on the results of visual observations was

estimated to be about 450–700 km, which is over 1.5 times longer than the calculated value for the ice SB. Therefore, the hypothesis of the ice origin of the Tunguska SB, which enters the atmosphere at an angle $\beta = 30^\circ$–40°, is hardly justified from this point of view.

Moreover, Fig. 12 shows the decrease in the mass of the ice SB with an initial radius of 100 m along the trajectory at small angles of entry into the atmosphere. As can be seen from the figure, the passage of the ice SB through the atmosphere while preserving a significant fraction of mass is possible only at a minimum altitude above 40 km, which contradicts with the estimated minimum altitude of about 10–15 km in the Tunguska event.

Our calculations showed that the trajectory length of the ice SB when it passes through the atmosphere at a minimum altitude of 15.5 km and small entry angles (less than 15°) until the moment of its complete loss of mass even at a radius of 100 m is two times shorter compared to the case of the iron SB. Thus, the through passage of the ice SB at small entry angles with a minimum trajectory altitude 10–15 km is impossible.

For the ice SB with a radius of 25 m, the length of the trajectory to the moment of the total loss of mass is reduced by four to five times. In addition, it was shown that a considerable part of the initial mass is preserved by iron and stone SBs with radii of 100, 50, and 25 m at an entry angle of 30°. But their fall would be accompanied by the formation of craters with a diameter larger than 1 km and a depth over 200 m.

As the final comments, which can be considered as the plan for future research, we can mention the following problems. In our work, we did not deal with the problem of the formation of a shock wave, although when comparing the Tunguska phenomenon with the Chelyabinsk meteorite with a size of about 10 m and an altitude of maximum energy release of about 30 km, we have no reason to doubt that the body that is 10–20 times larger with an altitude of maximum energy release of 10–15 km at a velocity of 20 km s^{-1} will create a shock wave with a huge amplitude and destructive force, capable of causing tree-fall over an area exceeding 1600 km^2. Experimental modelling of the knock-down effect of a shock wave from the source with cylindrical geometry was performed by Zotkin & Tsikulin (1966). The cylindrical source of the shock wave was modelled by a long detonating cord inclined at a certain angle to a plane planted with small sticks, which imitated trees in the Siberian forest. It was shown that the shape of the area of fallen sticks was similar to the shape of real tree-fall territory. However, Zotkin & Tsikulin (1966) did not model the dependence of the strength of the cylindrical shock wave on the height of its source above the ground. Instead, they added a point explosive at the lower end of their cord to model a presumed spherical component of the shock wave. Because rates of the mass and energy losses of the SB that caused the Tunguska event depend strongly on its altitude above the ground (as evident from Fig. 7), a sharp increase in energy release close to the minimum altitude reached by the through passing SB can be interpreted as an explosion creating a spherical component of the shock wave. Clearly, making a detailed prediction for the patterns of tree-fall in the framework of our hypothesis of a through-passed SB as a cause for the Tunguska event will be an important subject of future research.

In solving the main problems in this work, we confined ourselves to the need to make an upper estimate for calculating the residual mass of space body using the parameters maximizing the mass-loss. Finally, in this paper, we did not consider the problem of the mass-loss of the space body due to its fragmentation. This will be the subject of future research and the results will be published elsewhere (Khrennikov et al. 2020).

5 SUMMARY

Based on the obtained results, we can make the following statements:

(i) The conditions for the possible through passage of a large space body composed of various materials across the Earth's atmosphere with a minimal loss of mass and without collision with the surface of the planet are established. It was shown that this corresponds to the entry angles of space body into the atmosphere $\beta \leq 11^\circ.5$.

(ii) It was shown that the Tunguska space body could hardly consist of ice, since the length of the trajectory of such a body in the atmosphere before the complete loss of its mass would be less than the length of its trajectory estimated on the basis of observational data. This statement is valid for estimates performed for the value of the radiation heat transfer coefficient $c_h = 0.1$ as well as making allowance for uncertainties and variations of the values mentioned in the literature.

(iii) The value of the angle of entry into the atmosphere of 30°–40° mentioned in the literature for the Tunguska space body looks unrealistic, since it corresponds to the trajectory of a fall of a body with a large residual mass and trajectory length, which is 1.5–2 times shorter than the estimated trajectory length based on the observational data. Such a fall would be accompanied by the formation of a large crater, absent near the epicentre and around.

(iv) Probably, the most realistic version explaining the Tunguska phenomenon is the through passage of the iron asteroid body as the most resistible to fragmentation across the Earth's atmosphere at a minimum altitude of 10–15 km with the length of the trajectory in the atmosphere of about 3000 km and a subsequent exit of this asteroid body into the outer space to the near-solar orbit. This version is supported by the fact that there are no remnants of this body and craters on the surface of the Earth. Within this version, we can explain optical effects associated with a strong dustiness of high layers of the atmosphere over Europe, which caused a bright glow of the night sky.

If we admit the version of the complete loss of mass of SB after the passage of the epicentre or close to it, then the evidence of its reality would be the presence of droplets of meteoric iron of millimetre sizes on the Earth's surface along the trajectory of SB and around. It follows from Fig. 8 that the smaller the SB size and its mass are, the faster it loses a velocity (the amplitude of the shock wave near the epicentre also becomes smaller). Finally, when the velocity of a diminishing SB reduces to such an extent that its surface temperature approaches 1000°C, the sublimation ceases and the dominant mechanism of mass-loss consists of blowing off a liquid film from the surface of the body. In this case, the SB becomes the source of a huge amount of droplets, which will be sprayed by the SB. However, such microformations have not been found despite intensive searches around the epicentre and far beyond. The absence of iron droplets around the epicentre is explained by the high velocity of the SB during through passage across the Earth' s atmosphere – always over 11.2 km s^{-1} when the surface temperature exceeds several thousands of degree Celcius. The dominant mechanism of mass-loss at these temperatures is the sublimation of material in the form of single atoms, which can be found on the Earth's surface as iron oxides, which do not differ from the same widespread iron oxides of terrestrial origin.

ACKNOWLEDGEMENTS

Authors thank A. B. Klyuchantsev for aerodynamic calculations with the software package ANSYS FLUENT. The manuscript benefited from many suggestions and comments made in the constructive report by the reviewer, Dr Darrel Robertson, whom we thank for careful reading of the manuscript. We are grateful to Doug Black of Hamilton, Canada, for correcting the English in the final version of the manuscript.

REFERENCES

Ahrens T. J., O'Keefe J. D., 1972, The Moon, 4, 214
Andruschenko V. A., Syzranova N. G., Shevelev Y. D., 2013, Comput. Res. Model., 5, 927
Barri N., 2010, Arch. Comput. Methods Eng., 17, 1
Bronshten V. A., 1983, Physics of Meteoric Phenomena. Springer, Reidel
Bronshten V. A., 2000a, Planet. Space Sci., 48, 855
Bronshten V. A., 2000b, A&A., 359, 777
Chirikhin A. V., 2011, The Flow of Condensed and Dusty Media in the Nozzles of the Wind Tunnels. Fizmatlit, Moscow
Dudorov A. E., Badyukov D. D., Zamozdra S. N., Gorkavyi N. N., Eretnova O. V., Khaibrakhmanov S. A., Mayer A. E., Taskaev S. V., 2015, Mater. Sci. Forum, 845, 273
Farinella P., Foschini L., Froeschlé C., Gonczi R., Jopek T. J., Longo G., Michel P., 2001, A&A, 377, 1081
Fesenkov V. G., 1962, SvA, 38, 577
Gladysheva O., 2008, Tunguska Disaster: Puzzle Details. Lema, St. Petersburg
Hawkins G. S., 1964, The Physics and Astronomy of Meteors, Comets, and Meteorites. McGraw-Hill Series in Undergraduate Astronomy. McGraw-Hill , New York
Hutton D., 2017, Fundamentals of Finite Element Analysis. Tata McGraw-Hill, India
Johnson C. O., Stern E. C., Wheeller L. F., 2018, Icarus, 309, 25
Khrennikov D. E., Titov A. K., Ershov A. E., Klyuchantsev A. B., Pariev V. I., Karpov S. V., 2020, MNRAS, 493, 1352
Kundt W., 2003, Chin. J. Astron. Astrophys., 3, 545
Kutateladze S. S., 1990, Heat Transfer and Hydrodynamic Resistance. Energoatomizdat, Moscow
Loh W. H. T., 1963, Dynamics and Thermodynamics of Planetary Entry. Prentice-Hall, Upper Saddle River, NJ
Luchinsky G. P., 1985, Course of Chemistry. Vysshaya shkola, Moscow
Martin J. J., 1966, Atmospheric Entry — An Introduction to Its Science and Engineering. Prentice-Hall, Upper Saddle River, NJ
Morrison D., Robertson D. K., 2019, Icarus, 327, 1
NASA, 1976, U.S. Standard Atmosphere. U.S. Government Printing Office, Washington, DC
Nemchinov I. V., Popova O. P., Teterev A. V., 1999, J. Eng. Phys. Thermophys., 72, 1194
Robertson D. K., Mathias D. L., 2019, Icarus, 327, 36
Spearman L. M., Braswell D. O., 1993, Aerodynamics of a Sphere and an Oblate Spheroid for Mach Numbers from 0. 6 to 10.5 Including Some Effects of Test Conditions. NASA Technical Memorandum 109016, NASA Langley Research Center, Hampton, Virginia
Stulov V., Titova L. Y., 2001, Sol. Syst. Res., 35, 315
Stulov V. P., Mirskiy V. N., Vyslyi A. I., 1995, Aerodynamics of Bolides. Nauka, Moscow
Svetsov V. V., Nemtchinov I. V., Teterev A. V., 1995, Icarus, 116, 131
Tom Gehrels E., 1994, Hazards Due to Comets and Asteroids. Univ. Arizona Press, Tucson, Arizona
Voitkovskiy K. F., 1999, Fundamentals of Glaciology. Nauka, Moscow
Zhdan I. A., Stulov V. P., Stulov P. V., Turchak L. I., 2007, Sol. Syst. Res., 41, 505
Zotkin I. T., Tsikulin M. A., 1966, Dokl. Akad. Nauk SSSR, 167, 59

This paper has been typeset from a TEX/LATEX file prepared by the author.